

AD-A074 812 NAVAL ENVIRONMENTAL PREDICTION RESEARCH FACILITY MON--ETC F/6 4/2
A PRELIMINARY ANALYSIS OF MESOSCALE EFFECTS OF TOPOGRAPHY ON TR--ETC(U)
JUL 79 S BRAND, R P CHAMBERS, H J WOO
UNCLASSIFIED NEPRF-TR-79-04 NL

OF
AD
A074812





LEVEL

12

NAVENVPREDRSCHFAC
TECHNICAL REPORT
TR 79-04

NAVENVPREDRSCHFAC TR 79-04

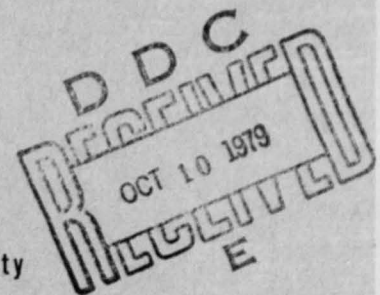
ADA074812

A PRELIMINARY ANALYSIS OF MESOSCALE EFFECTS OF TOPOGRAPHY ON TROPICAL CYCLONE-ASSOCIATED SURFACE WINDS

S. Brand and R. P. Chambers
Naval Environmental Prediction Research Facility

H. J. C. Woo, J. E. Cermak and J. J. Lou
Colorado State University

M. Danard
University of Waterloo



DDC FILE COPY

JULY 1979

APPROVED FOR PUBLIC RELEASE
DISTRIBUTION UNLIMITED

79 10 10 018



NAVAL ENVIRONMENTAL PREDICTION RESEARCH FACILITY
MONTEREY, CALIFORNIA 93940

Qualified requestors may obtain additional copies from the Defense Documentation Center. All others should apply to the National Technical Information Service.

UNCLASSIFIED

SECURITY CLASSIFICATION OF THIS PAGE (When Data Entered)

REPORT DOCUMENTATION PAGE		READ INSTRUCTIONS BEFORE COMPLETING FORM	
1. REPORT NUMBER <u>NAVENVPREDRSCHFAC</u>		2. GOVT ACCESSION NO.	
Technical Report TR 79-04		3. RECIPIENT'S CATALOG NUMBER	
4. TITLE (and Subtitle)		5. TYPE OF REPORT & PERIOD COVERED	
(6) A Preliminary Analysis of Mesoscale Effects of Topography on Tropical Cyclone-Associated Surface Winds		(9) Final rept.	
7. AUTHOR(s)		8. CONTRACT OR GRANT NUMBER(s)	
(10) S./Brand, R. P./Chambers* H.J.C./Woo, J.E./Cermak, & J.J./Lou** M. Danard***			
9. PERFORMING ORGANIZATION NAME AND ADDRESS		10. PROGRAM ELEMENT, PROJECT, TASK AREA & WORK UNIT NUMBERS	
Naval Environmental Prediction Research Facility, Monterey, CA 93940		PE 62759N, PN WF52551792 NEPRF W.U. 6.2-14	
11. CONTROLLING OFFICE NAME AND ADDRESS		12. REPORT DATE	
Naval Air Systems Command Department of the Navy Washington, DC 20361		(11) July 1979	
14. MONITORING AGENCY NAME & ADDRESS (if different from Controlling Office)		13. NUMBER OF PAGES	
(16) F52551		42 (12) 42	
(17) WF52551792		15. SECURITY CLASS. (of this report)	
		UNCLASSIFIED	
16. DISTRIBUTION STATEMENT (of this Report)		15a. DECLASSIFICATION/DOWNGRADING SCHEDULE	
Approved for public release; distribution unlimited.			
(14) NEPRF-TR-79-04			
17. DISTRIBUTION STATEMENT (of the abstract entered in Block 20, if different from Report)			
18. SUPPLEMENTARY NOTES			
Authors' affiliations: * Naval Environmental Prediction Research Facility ** Colorado State University, Ft. Collins, CO *** University of Waterloo, Ontario, Canada			
19. KEY WORDS (Continue on reverse side if necessary and identify by block number)			
Tropical cyclones Subic Bay, RP Mesoscale modeling			
20. ABSTRACT (Continue on reverse side if necessary and identify by block number)			
An analysis is made of the influence of topography on tropical cyclone-associated strong surface wind conditions for Subic Bay, Republic of the Philippines, by means of an environmental wind tunnel. Surface flow patterns were deduced by smoke and surface oil films, while isotach and gust values were obtained by hot wire anemometers. Laboratory results show the significant effects of the mountainous regions surrounding the Subic Bay harbor complex			

DD FORM 1473
1 JAN 73
(Page 1)EDITION OF 1 NOV 68 IS OBSOLETE
S/N 0102-014-6601

UNCLASSIFIED

SECURITY CLASSIFICATION OF THIS PAGE (When Data Entered)

407 279

JOB

UNCLASSIFIED

SECURITY CLASSIFICATION OF THIS PAGE(When Data Entered)

20. Abstract (Continued)

and indicate preferred shelter locations. These results are compared with synoptic observations and a high-resolution (0.19 n mi) diagnostic, one-level, primitive equation model. Where direct comparisons can be made, all techniques appear to show qualitative agreement.

DD Form 1473
1 Jan 73
S/N 0102-014-6601

UNCLASSIFIED

SECURITY CLASSIFICATION OF THIS PAGE(When Data Entered)

CONTENTS

1. INTRODUCTION	1
2. LABORATORY MODEL AND RESULTS	3
2.1 Laboratory Model	3
2.2 Results	6
2.2.1 Mean Winds	6
2.2.2 Maximum Gustiness	9
2.2.3 Vertical Variation	11
3. SYNOPTIC ANALYSIS	13
4. DYNAMIC MODEL OUTPUT	17
5. SUMMARY AND RECOMMENDATIONS	20
REFERENCES	23
ACKNOWLEDGMENTS	24
APPENDIX A - STREAMLINE-ISOTACH DISTRIBUTIONS	25
APPENDIX B - STREAMLINE AND MAXIMUM GUST DISTRIBUTIONS	33

Accession For	
NTIS GRA&I	<input checked="checked" type="checkbox"/>
DDC TAB	<input type="checkbox"/>
Unannounced	<input type="checkbox"/>
Justification	
By _____	
Distribution/	
Availability Codes	
Dist.	Availand/or special
A	

1. INTRODUCTION

In May 1976, Tropical Storm Olga drifted slowly westward across the Philippines and essentially stalled some 75 n mi north-northwest of Subic Bay, one of the major U.S. Navy installations in the western North Pacific. As this rather weak tropical cyclone (maximum winds of 40 kt) contributed southwesterly winds into Subic Bay, the vulnerability of vessels within the harbor became evident. With maximum surface winds of only 35-45 kt observed in the harbor, five Navy ships sustained light to moderate hull damage and became part of the total \$1.4 million damage to ship and harbor facilities caused by TS Olga.

With the multitude of anchorages and pierside berths available, a major problem for ship commanders and other decision makers in Subic Bay was where to place vessels within the harbor complex so as to minimize stress on ship and port facilities. Knowledge of the streamline-isotach conditions within the harbor for winds coming from the vulnerable directions of south through west would certainly have aided the decision-making process.

The mesoscale nature of the problem is further complicated by the complex topography of the Subic Bay area (Figure 1). The bay is surrounded by mountainous terrain to the west, northeast, and southeast, with passes through the mountains to the east-northeast and northwest.

In order to simulate in a laboratory setting the surface streamline-isotach distributions throughout the harbor, a scale model of the Subic Bay area was constructed at the Fluid Dynamics and Diffusion Laboratory (FDDL) at Colorado State University. The information derived from this experiment was compared with synoptic analyses of strong southwesterly wind situations observed at Subic Bay. The experiment results also were compared independently with the results of a high resolution primitive equation model designed for the Subic Bay area.

This report presents the finding of these independent analyses, in order to provide guidance to decision makers who must plan for tropical cyclone stress conditions in the Subic Bay area.

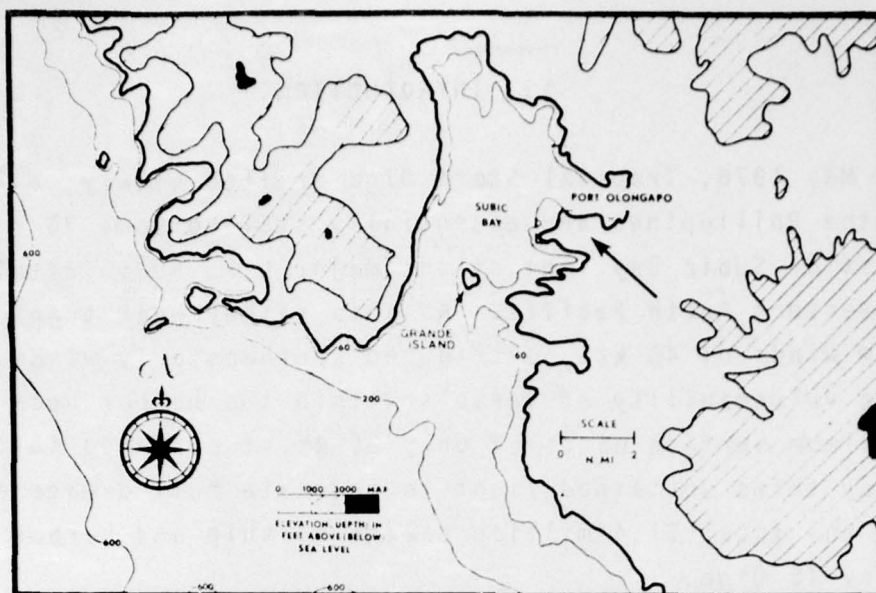


Figure 1. Subic Bay area on the west coast of the Philippine Islands at $14^{\circ} 15' N$, $120^{\circ} 14' E$. Anchorages generally are available within the bay area for depths greater than 60 ft. Terrain topographical features and bottom contours shown in feet. Arrow points to Cubi Point Runway.

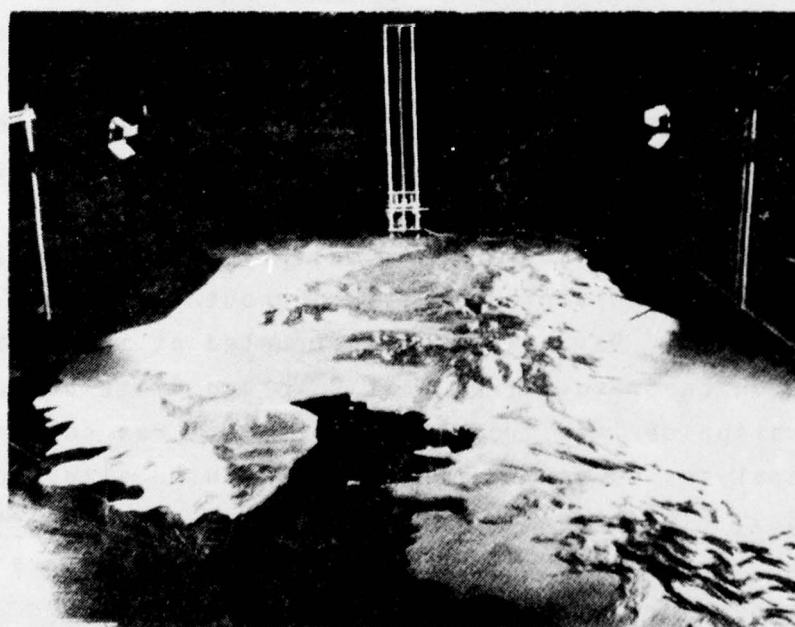


Figure 2. Topographical model in wind tunnel, viewed from the south. Grid squares in bay area are four inches on a side and relate to 0.82 n mi squares.

2. LABORATORY MODEL AND RESULTS

2.1 LABORATORY MODEL

The 1:15,000 scale model of the Subic Bay area used in the experiment is shown in Figure 2. The terrain was constructed from styrofoam sheets cut to match contour lines of the topography; surfaces were smoothed with clay and painted. The model was studied in the Fluid Dynamics and Diffusion Laboratory's environmental wind tunnel, shown in Figure 3.

The study included flow visualization using oil films and smoke (titanium tetrachloride), as well as hot-wire anemometer measurements. Rotation of the scale model facilitated development of surface flow patterns, mean wind speed isotachs, and gustiness values for the entire Subic Bay area for incoming wind directions from south through west (15° intervals). For more details on the experimental technique, the reader is referred to Woo et al., 1978.

Values of mean wind speed and turbulence intensity¹ (related to gustiness) were examined at four scale elevations -- .06, .12, .16 and .22 inches, representing heights in the real atmosphere of 70, 150, 195 and 275 ft, respectively -- for the 60 locations shown in Figure 4.

The mean wind speed and maximum gust profiles taken upstream of the bay entrance, are characteristic of the boundary layer upstream of the model. The boundary layer thickness δ was 2.5 inches, corresponding to a prototype of 3125 ft in the real atmosphere. The relationship to examine the vertical variation of the horizontal wind speed can be written as

$$\frac{U}{U_{\infty}} = \left(\frac{z}{\delta}\right)^n,$$

where U is the mean wind speed at level z , U_{∞} is the mean wind speed at the top of the boundary layer at height δ , and n is a

¹ Turbulence intensity, U_T , is related to mean wind speed, U and maximum gust, U_g , by: $U_g = U(2U_T + 1)$.

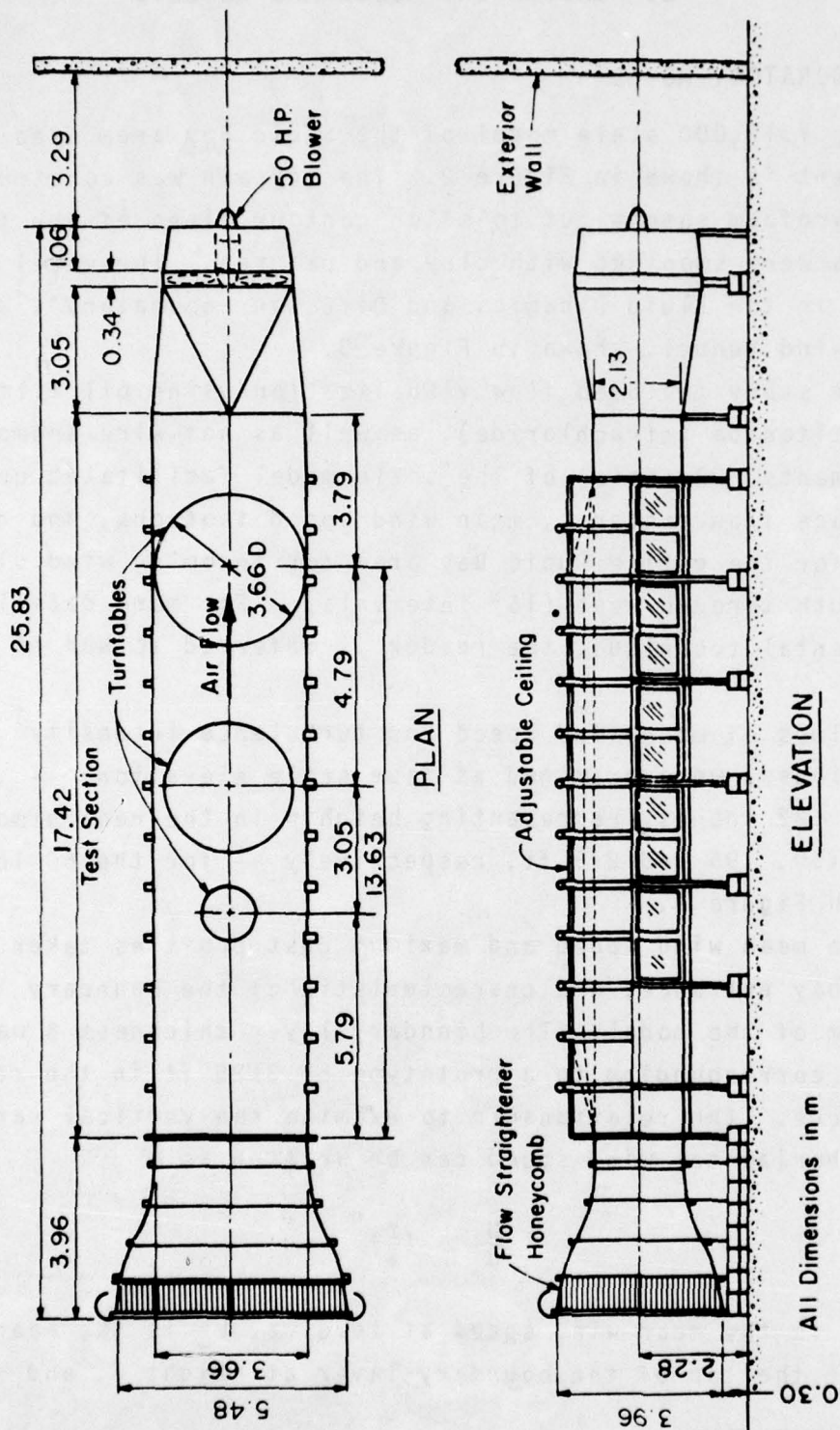


Figure 3. Environmental wind tunnel at the Fluid Dynamics and Diffusion Laboratory of Colorado State University.

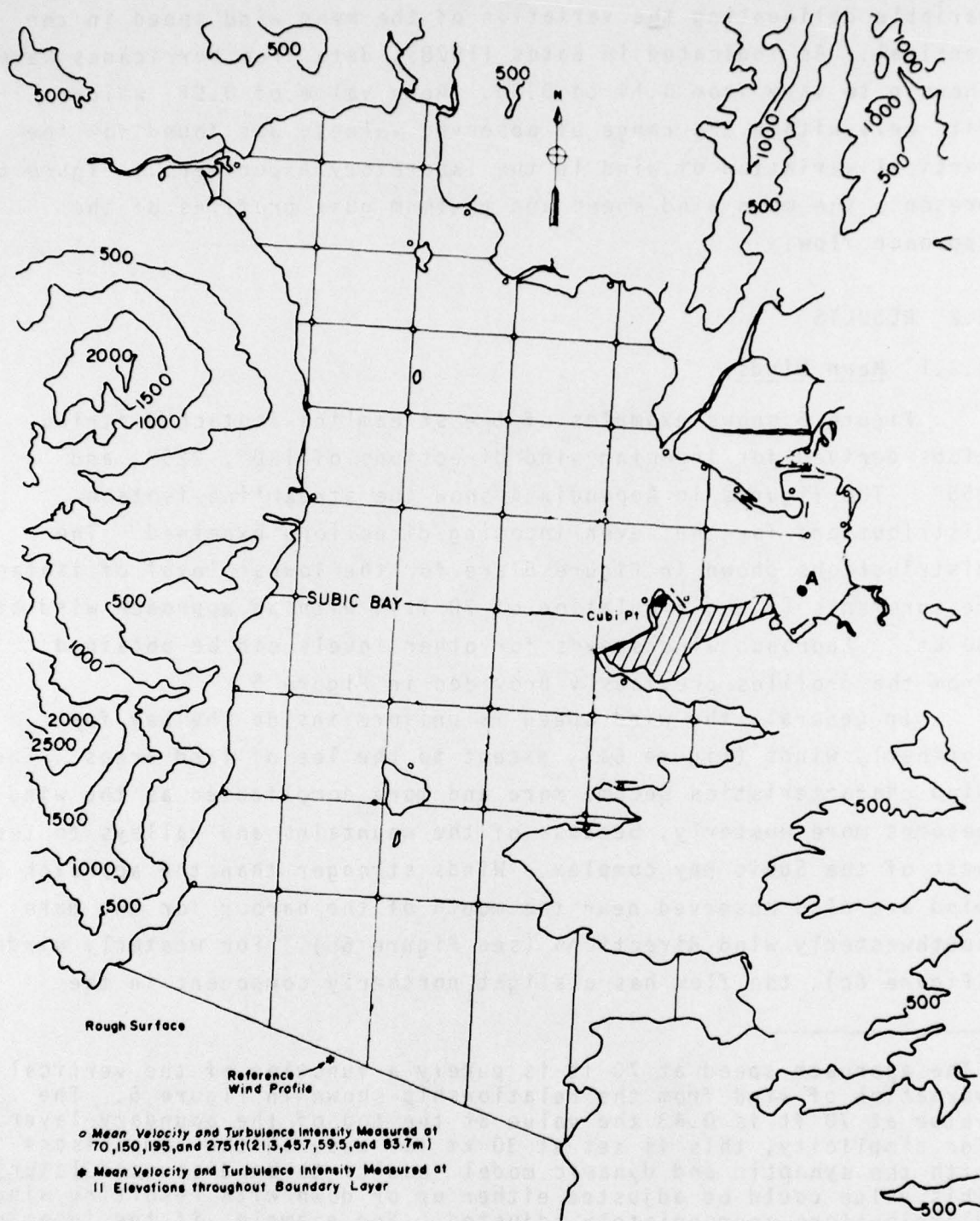


Figure 4. Measurement locations for wind speed and turbulence intensity. Topographical elevations shown in ft.

variable delineating the variation of the mean wind speed in the vertical. As indicated in Bates (1978), data from hurricanes have shown n to vary from 0.14 to 0.30. An n value of 0.22, which fits well within the range of observed values, was found for the vertical variation of wind in the laboratory experiment. Figure 5 presents the mean wind speed and maximum gust profiles of the approach flow.

2.2 RESULTS

2.2.1 Mean Winds

Figure 6 shows examples of the streamline-isotach distributions derived for incoming wind directions of 180° , 225° , and 255° . The figures in Appendix A show the streamline-isotach distributions for the seven incoming directions examined. The distributions shown in Figure 6 are for the lowest level of isotach measurements (i.e., simulation of 70 ft), with an approach wind of 30 kt.² Approach wind speeds for other levels can be obtained from the profiles previously provided in Figure 5.

In general, the wind speed is uniform inside the bay for southerly winds (Figure 6a), except to the lee of land areas. The wind characteristics become more and more complicated as the wind becomes more westerly, because of the mountains and valleys to the west of the Subic Bay complex. Winds stronger than the approach wind are also observed near the mouth of the harbor for the more southwesterly wind directions (see Figure 6b). For westerly winds (Figure 6c), the flow has a slight northerly component in the

²The approach speed at 70 ft is purely a function of the vertical variation of wind from the relationship shown in Figure 5. The value at 70 ft is 0.43 the value at the top of the boundary layer. For simplicity, this is set at 30 kt for ease in the comparisons with the synoptic and dynamic model results to be discussed later. This value could be adjusted either up or down with resulting wind distributions appropriately adjusted. For example, if the incoming wind is 45 kt rather than 30 kt, then the 20 kt isopleth within the harbor would become a 30 kt isopleth. The laboratory experiment was not performed at varied incoming wind speeds, but only at varied directions.

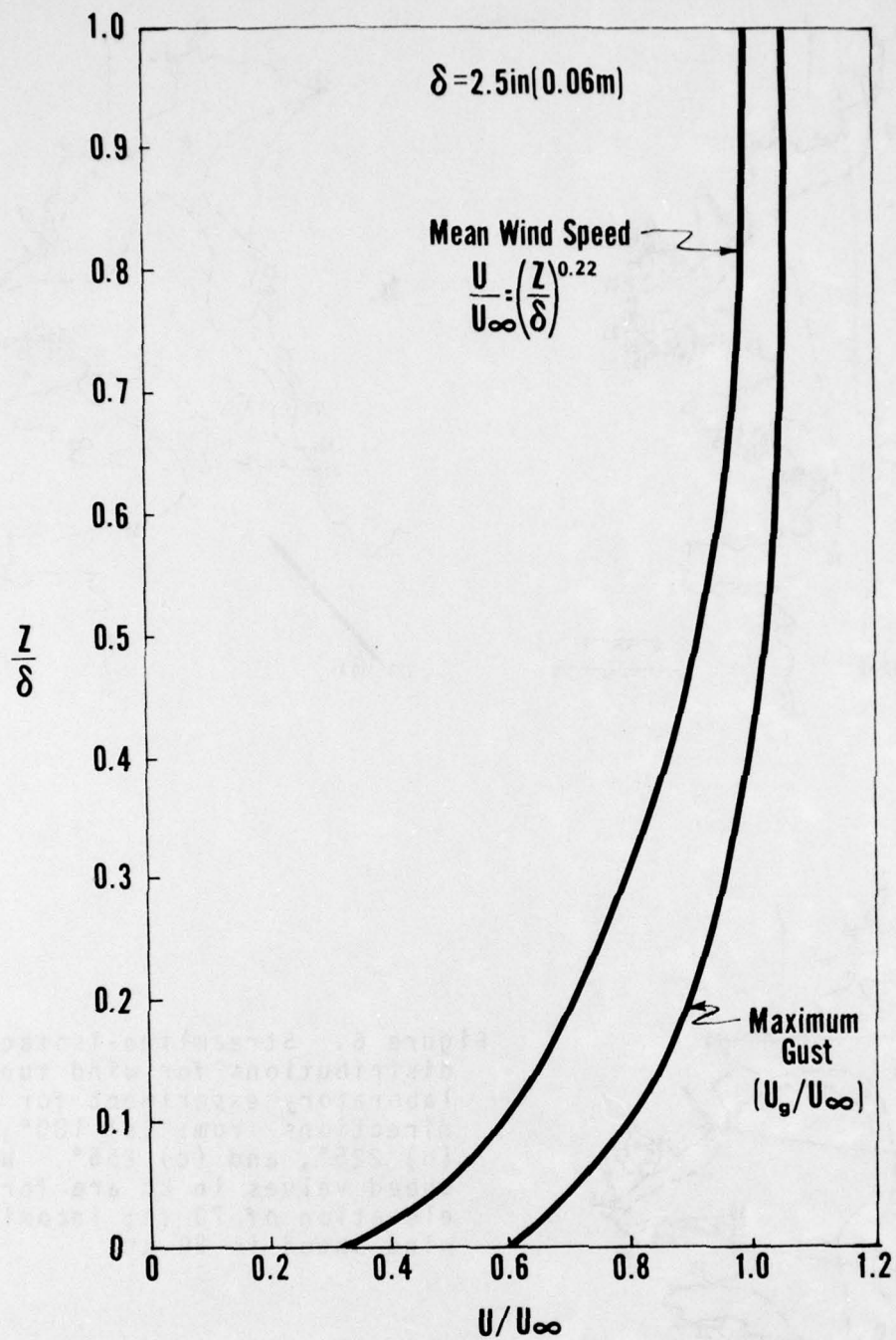


Figure 5. Mean wind speed and maximum gust profiles of the approach flow. U is the mean wind speed at level z , U_{∞} is the mean wind speed at the top of the boundary layer at height δ , and U_g is the maximum gust wind value.

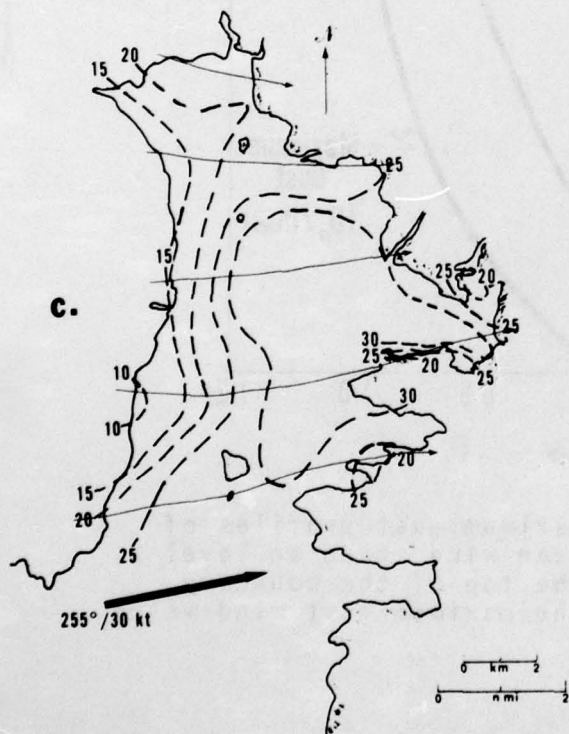
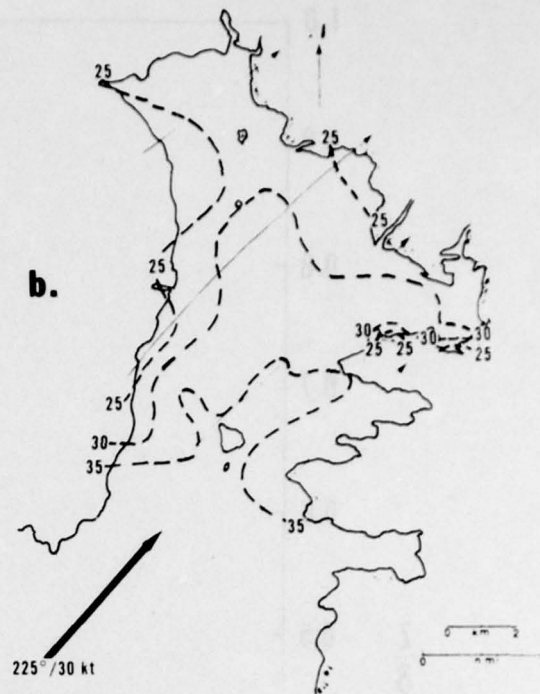
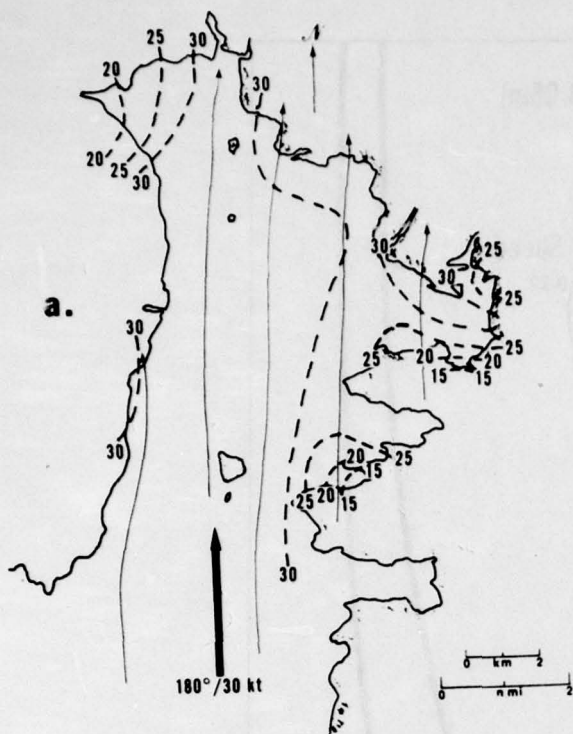


Figure 6. Streamline-isotach distributions for wind tunnel laboratory experiment for wind directions from: (a) 180°, (b) 225°, and (c) 255°. Wind speed values in kt are for an elevation of 70 ft; incoming wind speed is 30 kt.

upper section of the harbor. The mountains generally provide good sheltering for the region near the west of the bay when the wind approaches from behind the mountains, but this effect is not observed on the east side of the bay. In some cases winds even higher than the approach wind are observed due to converging secondary flows through the valleys between mountain peaks.

2.2.2 Maximum Gustiness.

As noted earlier, another application of the model results was the development of the capability to derive maximum gustiness values incorporating the mean wind and turbulence intensity measurements. For example, Figure 7 depicts (a) the mean wind of an approach flow of 255° at 30 kt and (b) the derived maximum gust values (highest wind over a one-minute period). Maximum gusts over 50 kt were observed in the central bay region. In the sheltered western portion of the harbor, maximum gust values were approximately twice the observed mean wind values. Near the harbor mouth, which is much less influenced by terrain than the interior of the Bay, the gust factor (gust value) was approximately 1.4 the mean wind value.

These figures can be compared with a tropical cyclone gust factor of 1.1 to 1.8 found by Gentry (1953) for the ratio of gust speed to five-minute mean speed. Shiotani (1975) found values ranging from 1.2 to 1.5 for a typhoon passage as observed by a meteorological tower. Atkinson and Holliday (1977) deduced a value of 1.25 for a maximum sustained 40 kt, one-minute wind speed for a tropical cyclone over water.

Ship commanders will sometimes find it more important to have knowledge of the gustiness associated with wind conditions than simply knowledge of a consistent strong wind. Commanders can adjust to consistent strong winds, but the variable forces of gustiness can be hazardous to a ship at anchor or at pierside. Analyses of the maximum gusts for the seven wind directions examined in the laboratory experiment are shown in Appendix B.

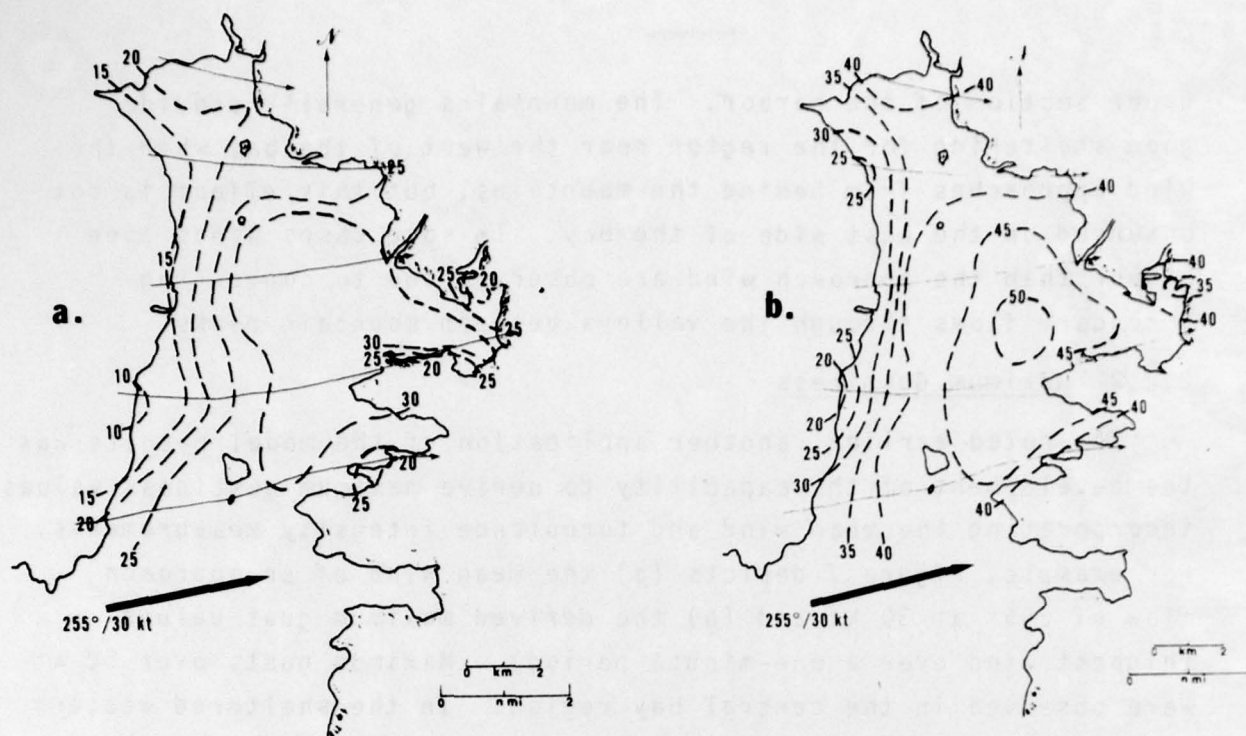


Figure 7. Streamline-isotach distributions for (a) an incoming wind from 255° at 30 kt and (b) the maximum gust values in kt. Both distributions are for the 70 ft elevation.

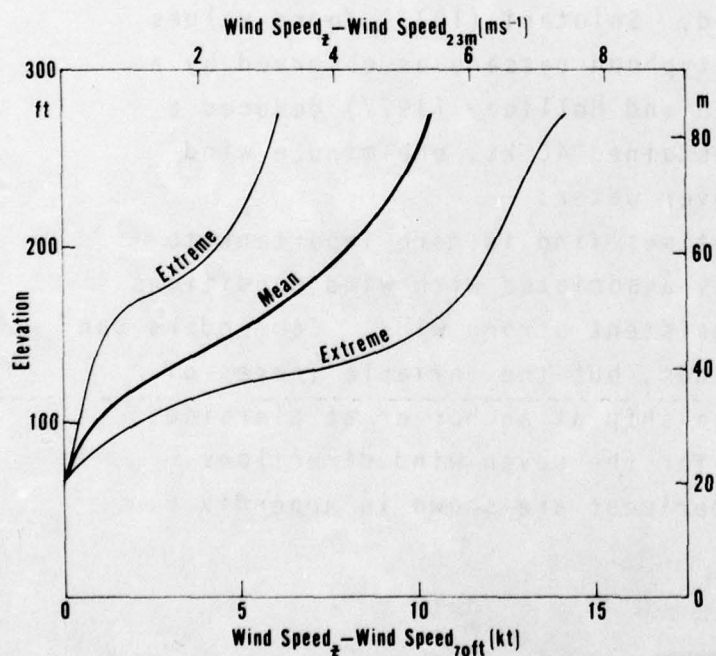


Figure 8. The vertical variation of wind at a point 1/3 n mi to the east-northeast of Cubi Point Runway, based on winds from south through west. The mean and extremes of the differences of the wind speed at any elevation Z , minus the wind at 70 ft are plotted for the vertical variation from 70 to 275 ft.

2.2.3 Vertical Variation

The vertical variation of wind and the turbulence associated with wind are important considerations in the structural design of large buildings and bridges in coastal regions and harbors likely to be affected by tropical cyclones. Personnel at coastal airport locations also must be aware of the vertical wind shear in the critical lowest few hundred feet under strong wind or typhoon stress conditions.

In the Subic Bay model experiment, the vertical variation of the wind throughout the harbor for each wind direction was deduced for the simulated boundary layer from 70 ft to 275 ft. An example of the vertical variation of the wind for one particular location (Point A in Figure 4) is shown in Figure 8. Assuming south-westerly winds, this location is downwind approximately $1/3$ mi from the end of Cubi Point runway.

3. SYNOPTIC ANALYSIS

In the wake of the damaging southwest winds generated by Tropical Storm Olga in May 1976, the Naval Weather Service Environmental Detachment at Cubi Point coordinated a data collection program within the Subic Bay area. The aim was to obtain extensive synoptic information from ships located throughout the harbor complex, whether at anchor or at pierside, during strong southwest wind conditions. During the period May 1976 through September 1977, five synoptic situations resulted in strong southwesterly winds: four were associated with tropical cyclones in close proximity (Tropical Storms Olga, 21-25 May 1976; Iris 14-16 September 1976; Sarah, 12 July 1977; and Dinah, 16 September 1977); and the fifth included a period of unusually strong monsoonal southwesterly winds (17 May 1977).

The data set included observations from ships as well as information from a recording weather station located near the airport runway at a height of approximately 70 ft (see Figure 9). Since ship anemometers vary considerably in elevation (for example, some carriers have their anemometers over 150 ft above mean sea level), all observations were normalized to the 70 ft elevation by the vertical variation of tropical cyclones discussed by Bates (1978). Figure 10 shows the normalized profiles for the vertical wind variation for tropical cyclones over land and over water as described by Bates. A mean value between these two curves was used in this segment of the study. The normalized profile for the approach flow of the laboratory model was very similar to the mean value of the land and water profiles.

Incoming or approach wind information was estimated from synoptic data provided by Fleet Numerical Weather Central, the National Meteorological Center, the Japan Meteorological Agency, the Royal Observatory at Hong Kong, and the Naval Weather Service Environmental Detachment at Cubi Point. This data base was supplemented by the wind distribution information contained in tropical cyclone warnings issued by the Joint Typhoon Warning Center, Guam.

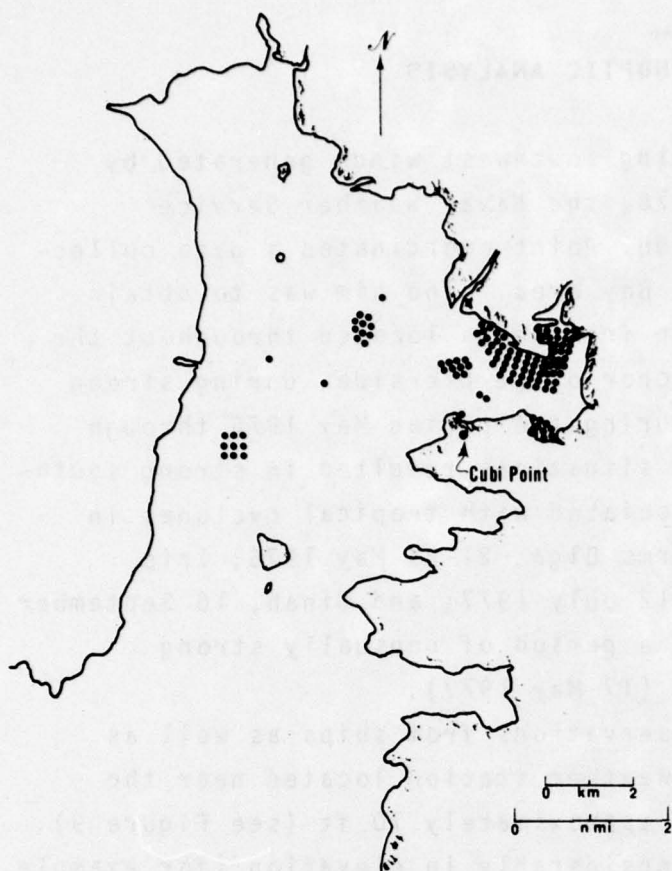


Figure 9. Distribution of synoptic observations from ships. In addition, 21 observations from Cubi Point recording station were incorporated. Incoming wind directions range from 225° to 255° .

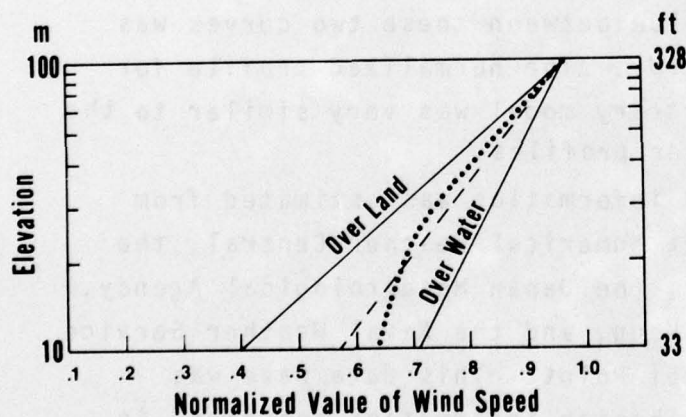


Figure 10. Normalized profiles of the variation of wind speed with height in the lowest boundary layer of tropical cyclones (after Bates, 1978). The dashed line indicates the relationship used for the present study. The dotted line indicates the normalized approach-flow profile for the laboratory model.

In order to simplify the analysis and presentation of results, estimated incoming winds (generally ranged from 25 to 35 kt) were normalized to a value of 30 kt. The resulting harbor winds were modified proportionally as appropriate. For example, if the incoming wind was 35 kt and reduced to 30 kt, a ship in the harbor reporting 20 kt would be proportionally reduced to 17.1 kt. Figure 11a shows the results of the synoptic analyses of composited data for incoming approach winds from 225°-255°. Figure 11b presents a laboratory model composite wind distribution based upon the incoming winds from 225°, 240° and 255° and drawn for the comparable 11a region.

The isotach maximum to the northwest of Cubi Point and the primary extension of the maximum to the east are evident in both Figures 11a and b. A secondary extension is also evident to the north in Figure 11a but is more pronounced in 11b. In addition, the decrease in winds toward the western shore is detectable in both figures. While these pattern similarities agree, the synoptic isotach values are generally less in magnitude, particularly to the north of the maximum and in the sheltered lee locations in the eastern section of the harbor. While a real difference might exist, some of the differences might be attributable to overestimates of the wind distribution in the tropical cyclone warnings. An overestimate of the wind distribution would contribute to an overestimate of the incoming wind. Since incoming wind and harbor winds were proportionally adjusted to an incoming wind of 30 kt, an overestimate of incoming wind would lead to a less than real harbor wind. In an examination of the effects of 30 typhoons crossing the Philippines, Brand and Blelloch (1973) found an average surface wind decrease of 33%. If the effects of the Philippines on the wind and wind distribution is not fully taken into account, the tropical cyclone warnings containing such information might be overestimated.

The comparison differences in the sheltered locations, if a real difference exists, might also reflect the necessity for a higher resolution laboratory model using output from the larger scale model as input.

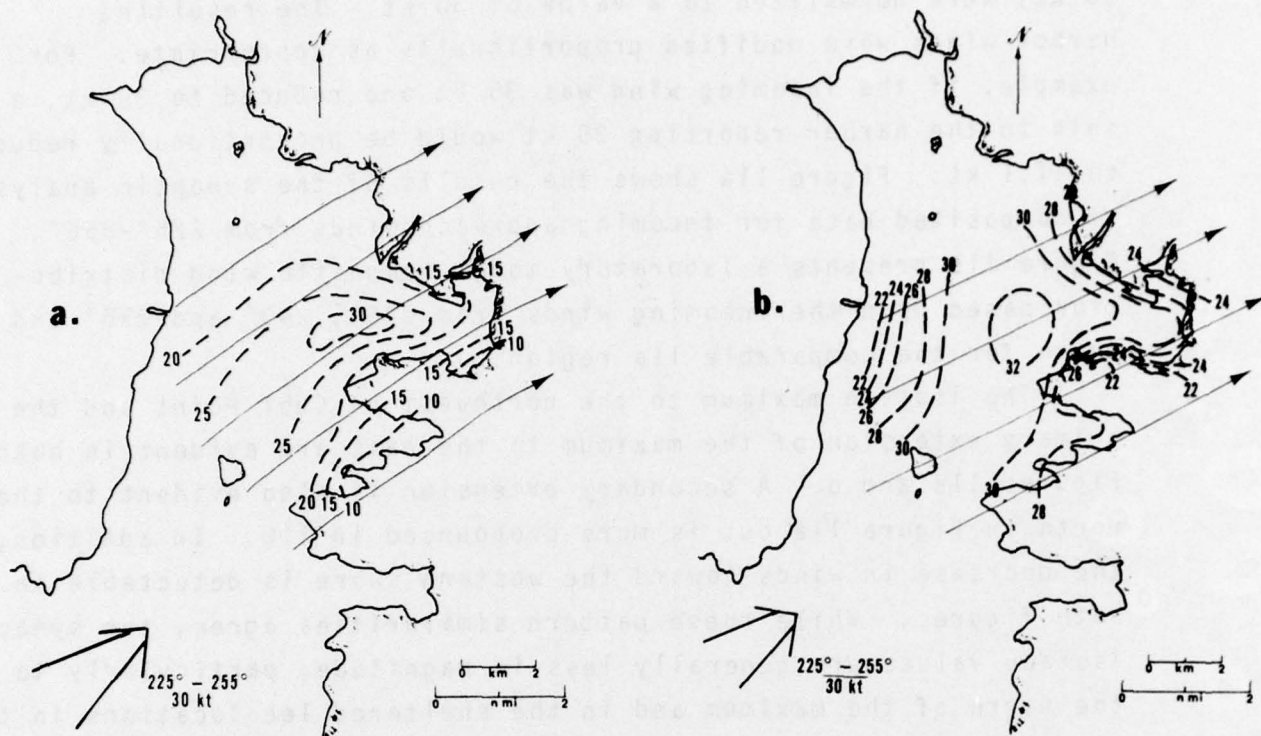


Figure 11. (a) Synoptic analysis of composited wind data (141 observations) normalized to 30 kt approach wind and 70 ft elevation; analysis is only over region where data were available, and is for the approach wind range 225°-255°. (b) Laboratory model composite wind distribution based upon the incoming winds from 225°, 240°, and 255°; analysis is only over the region shown in (a).

4. DYNAMIC MODEL OUTPUT

A diagnostic examination of the low-level surface wind field was also made by means of a one-level, primitive equation model which computes mesoscale influences of orography, friction and heating on surface winds, given large-scale synoptic data. The grid interval in the Subic Bay application was 0.19 n mi and the area covered was a 4.3 x 4.3 n mi region covering the eastern section of the bay.³

An example of one tropical cyclone case that was diagnostically examined is discussed. The resulting winds are for an elevation at approximately 70 ft. The planetary boundary layer of the model was assumed to be thoroughly mixed by mechanical turbulence and the drag coefficients used were 1.3×10^{-2} for land and 1.1×10^{-3} for water. The input winds at the top of the planetary boundary layer were 250° at 49 kt with resulting low-level winds of approximately 225° at 30 kt. Upper air temperatures were assumed to be similar to the mean typhoon temperatures of Bell and Kar-siung (1973).

For the experimental case examined, the results qualitatively compare well with the synoptic and laboratory wind distributions for similar low-level approach winds. The dynamic model results are limited to the eastern sector of the harbor and appear to show the isotach maximums extending toward the east over the water regions of the harbor (Figure 12a). The comparable synoptic composite of available data (Figure 12b) also shows this maximum to the east north of Cubi Point runway as does the laboratory results (Figure 12c). The wind maximum to the southwest of Cubi Point runway appears also to extend eastward for both the dynamic and laboratory distributions. For this particular wind comparison, synoptic data was not available to the southwest of Cubi Point.

³This model has previously been applied to the Juan de Fuca and Georgia Straits in British Columbia, using a 5.4 n mi grid size; see Danard (1977) for details.

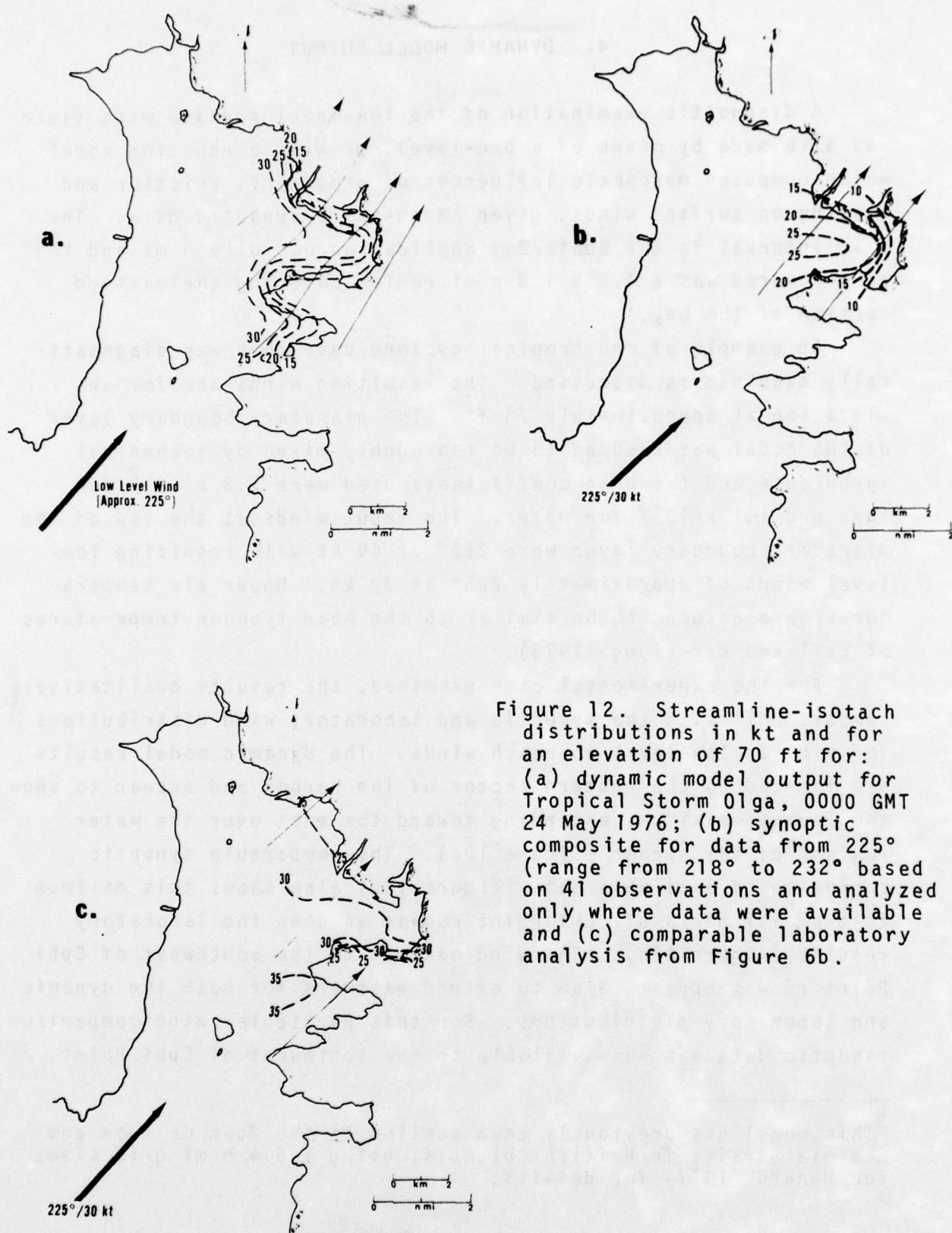


Figure 12. Streamline-isotach distributions in kt and for an elevation of 70 ft for: (a) dynamic model output for Tropical Storm Olga, 0000 GMT 24 May 1976; (b) synoptic composite for data from 225° (range from 218° to 232° based on 41 observations and analyzed only where data were available and (c) comparable laboratory analysis from Figure 6b.

Since the topography to the west of the bay has not been considered in these cases, it would be beneficial to run a larger scale model covering the whole domain and then use the output from this as the input for the higher resolution grid.

5. SUMMARY AND RECOMMENDATIONS

An attempt has been made to examine the low-level flow of a tropical cyclone in the vicinity of a harbor that is surrounded by complex terrain. Several approaches were used to deduce the streamline-isotach distributions as functions of incoming wind directions. Results of both the laboratory experiment and the dynamic model show promise. However, it is difficult to draw quantitative conclusions without a greater number of more detailed observations from both inside and outside the harbor. With a detailed observational network, the Subic Bay area would provide a setting for the necessary ground truth, especially since this major Department of Defense installation is threatened by an average of four tropical cyclones each year.

The mesoscale (in fact, almost microscale) nature of the problem is certainly challenging from the viewpoint that very little has been successfully achieved in the past on this diagnostic scale, although this is precisely the scale that seriously concerns many local forecasters, particularly under strong wind stress conditions. The approaches presented in this study should be further explored, insofar as they demonstrate potential applications to the many other harbors worldwide that are affected by tropical cyclones.

REFERENCES

- Atkinson, G. D. and C. R. Holliday, 1977: Tropical cyclone minimum sea level pressure/maximum sustained wind relationship for the western North Pacific. Mon. Wea. Rev., 105, 421-427.
- Bates, J., 1977: Vertical shear of the horizontal wind speed in tropical cyclones. NOAA Technical Memorandum ERL WMPO-39, 19 pp.
- Bell, G. J., and T. Kar-siung, 1973: Some typhoon soundings and their comparison with soundings in hurricanes. J. Appl. Meteor., 12, 74-93.
- Brand, S. and J. W. Blelloch, 1973: Changes in the characteristics of typhoons crossing the Philippines. J. Appl. Meteor., 12, 104-109.
- Danard, M., 1977: A simple model for mesoscale effects of topography on surface winds. Mon. Wea. Rev., 105, 572-581.
- Gentry, R. C., 1953: Wind velocities during hurricanes. Proc. Amer. Soc. of Civ. Eng., v. 79, 26 pp.
- Shiotani, M., 1975: Turbulence measurements at the seacoast during high winds. J. Met. Soc. Japan, 53, 340-354.
- Woo, H. G. C., J. E. Cermak and J. J. Lou, 1978: Wind characteristics over Subic Bay, Philippine Islands, during typhoon passage - Determination by physical modeling in a meteorological wind tunnel. NAVENVPREDRSCHFAC Contractor Report CR 78-02, 102 pp.

ACKNOWLEDGMENTS

The authors express their appreciation to Mr. J. R. Hurd for his assistance in data reduction, and for the assistance of Mr. C. D. Caron in model construction. The constructive comments of Dr. A. I. Weinstein of NEPRF are gratefully acknowledged.

APPENDIX A
STREAMLINE-ISOTACH DISTRIBUTIONS

Streamline-isotach distributions (in kt) from the wind tunnel laboratory experiment as a function of varying wind direction are shown in Figures A-1 through A-7. Wind speed values are for a 70 ft elevation; incoming wind speed is 30 kt.

<u>Figure Number</u>	<u>Wind Direction From</u>
A-1	180°
A-2	195°
A-3	210°
A-4	225°
A-5	240°
A-6	255°
A-7	270°

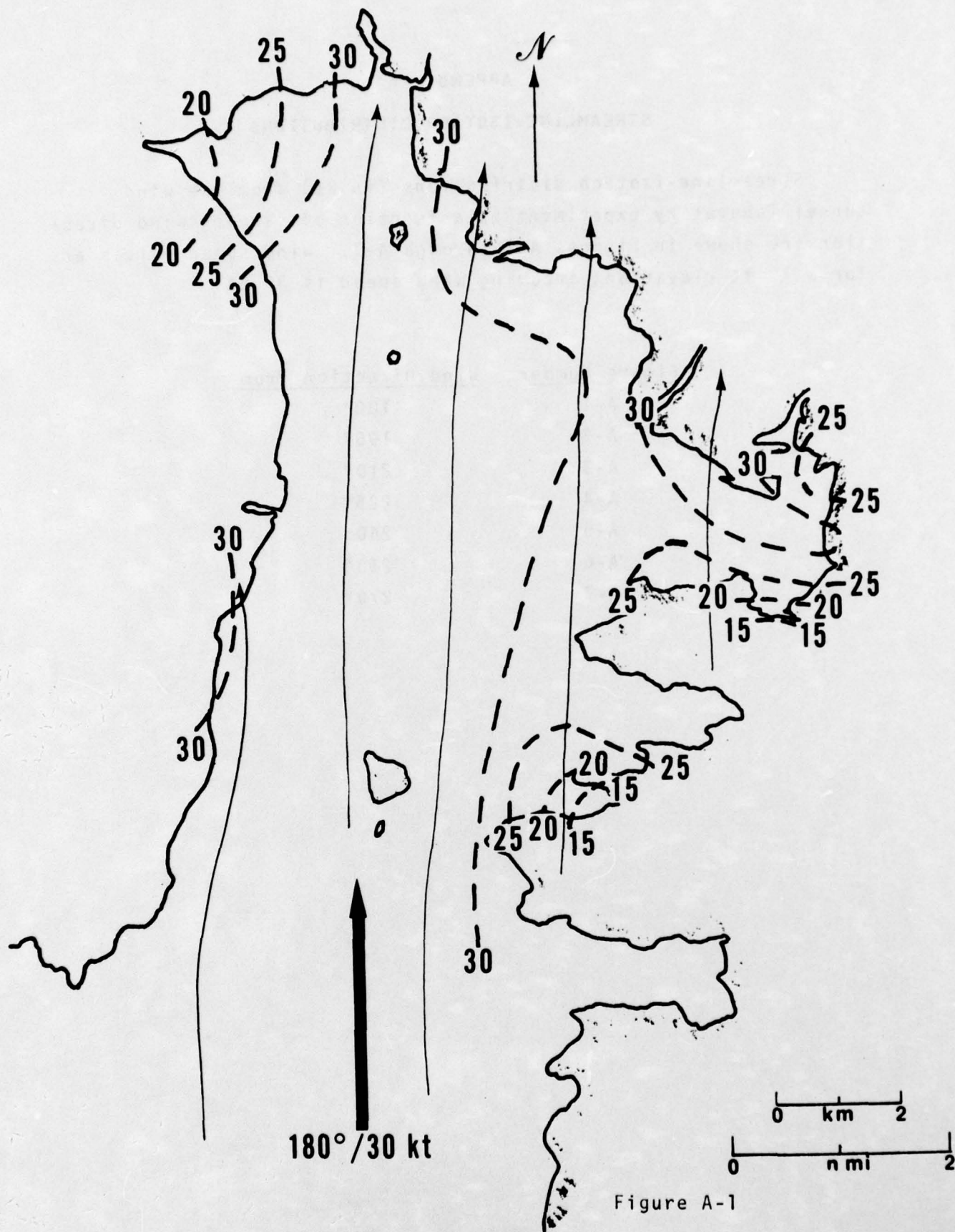


Figure A-1

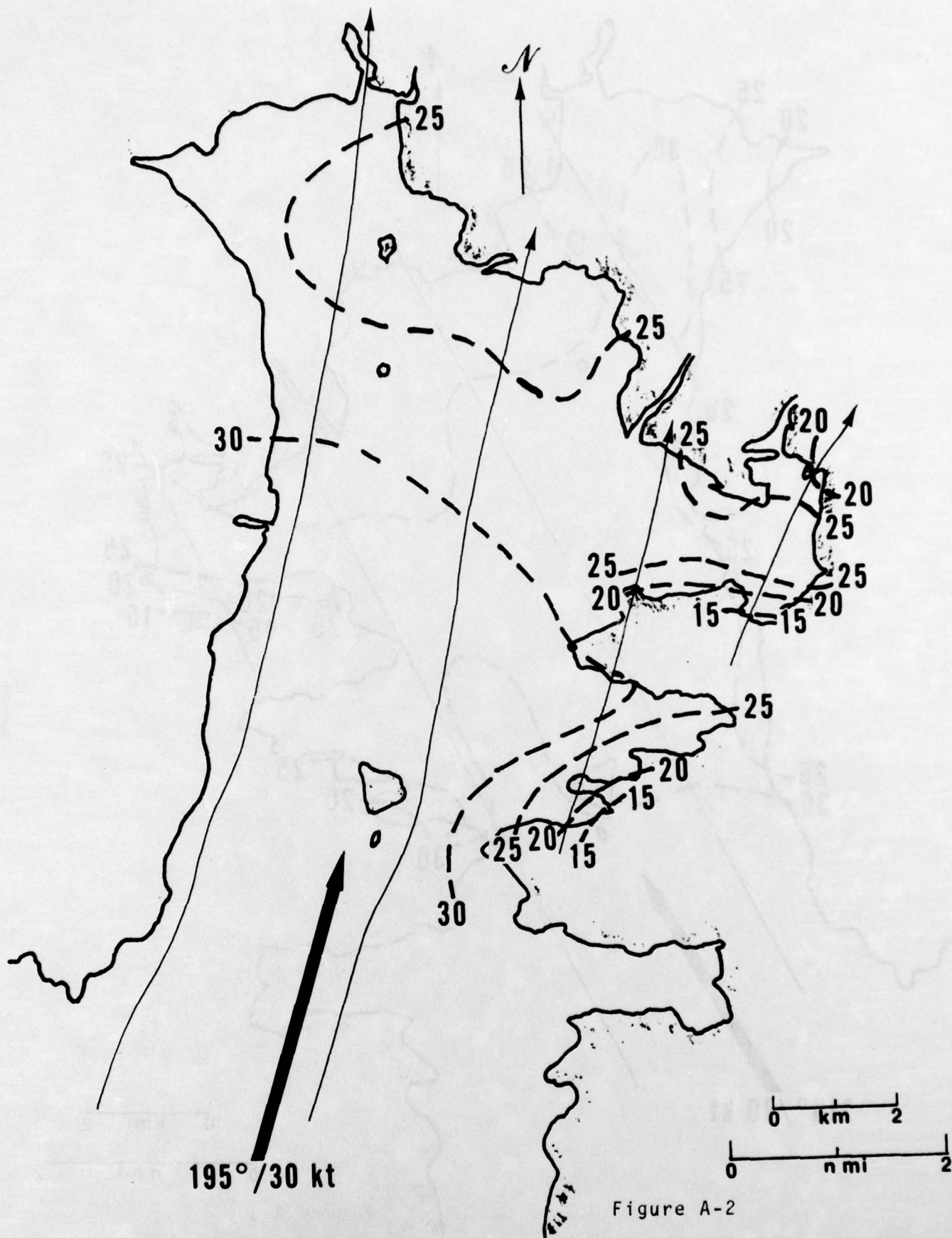
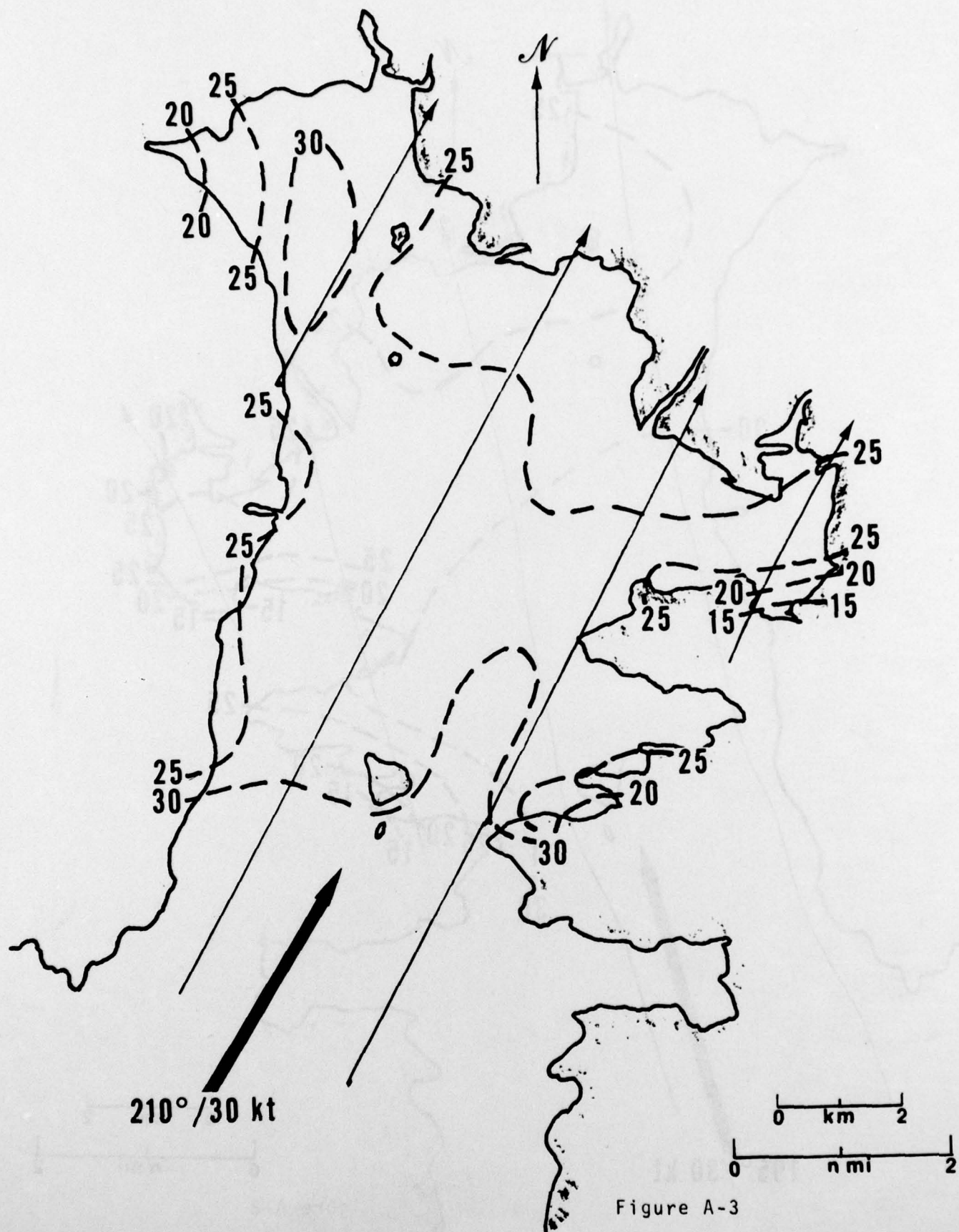


Figure A-2



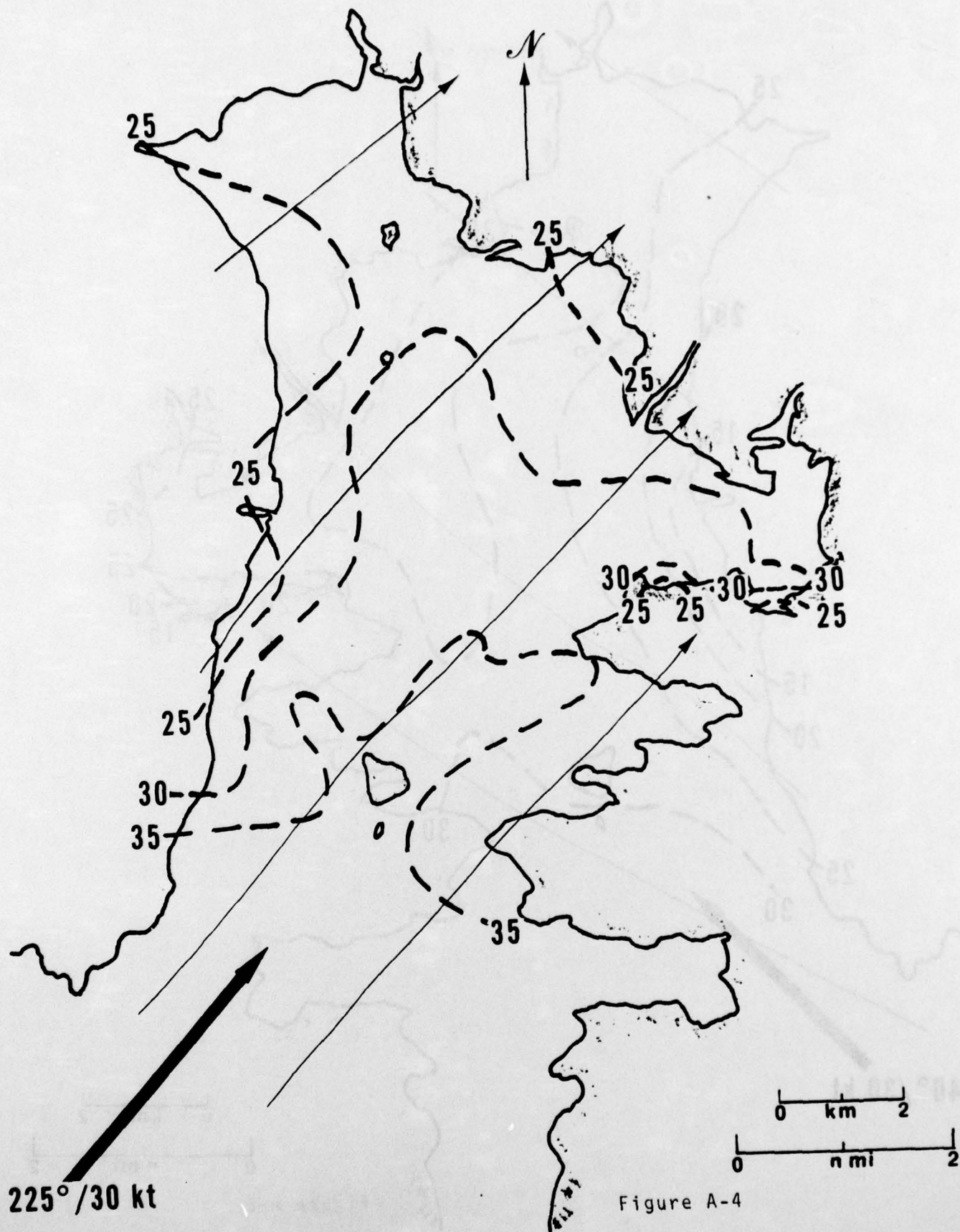


Figure A-4

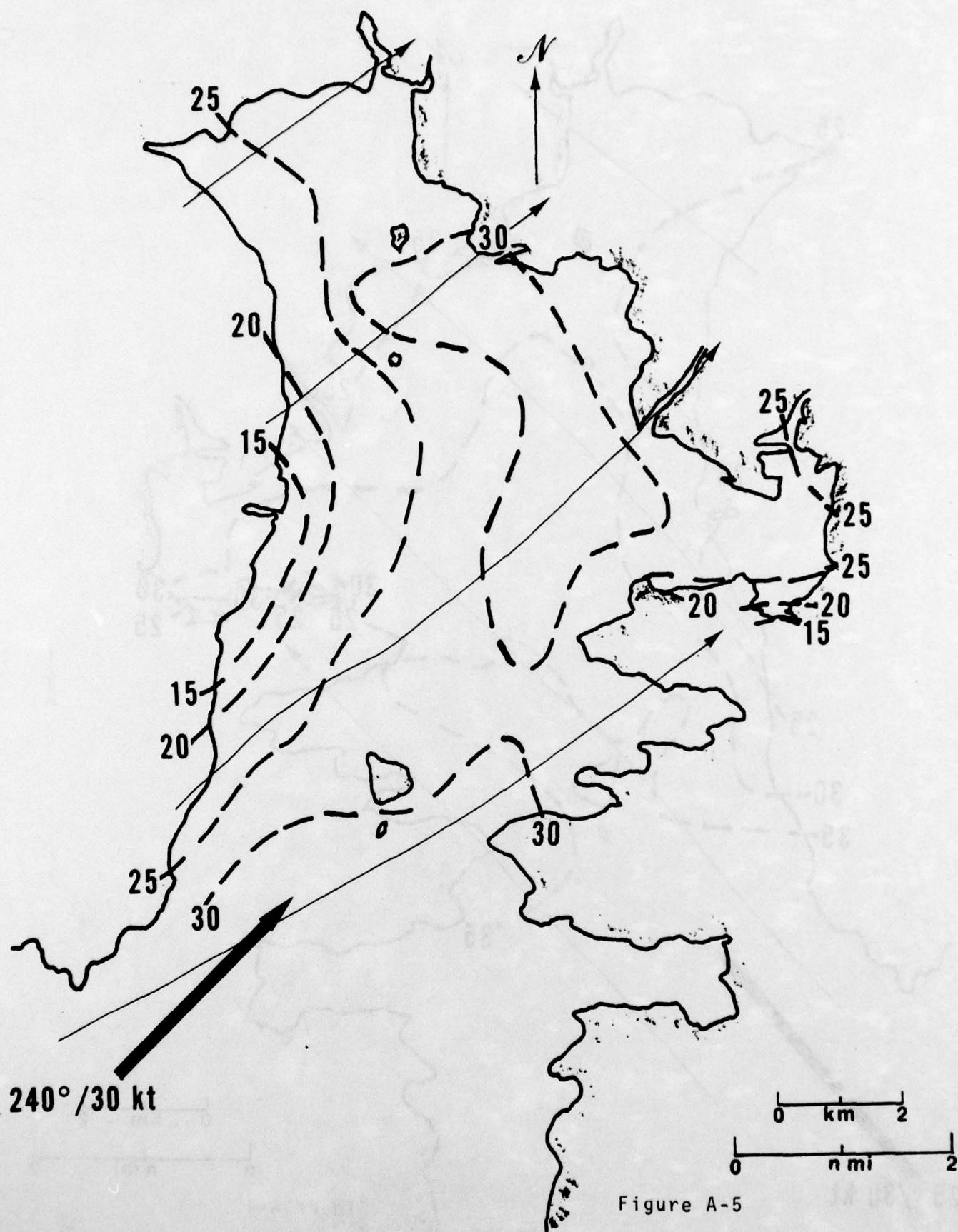


Figure A-5

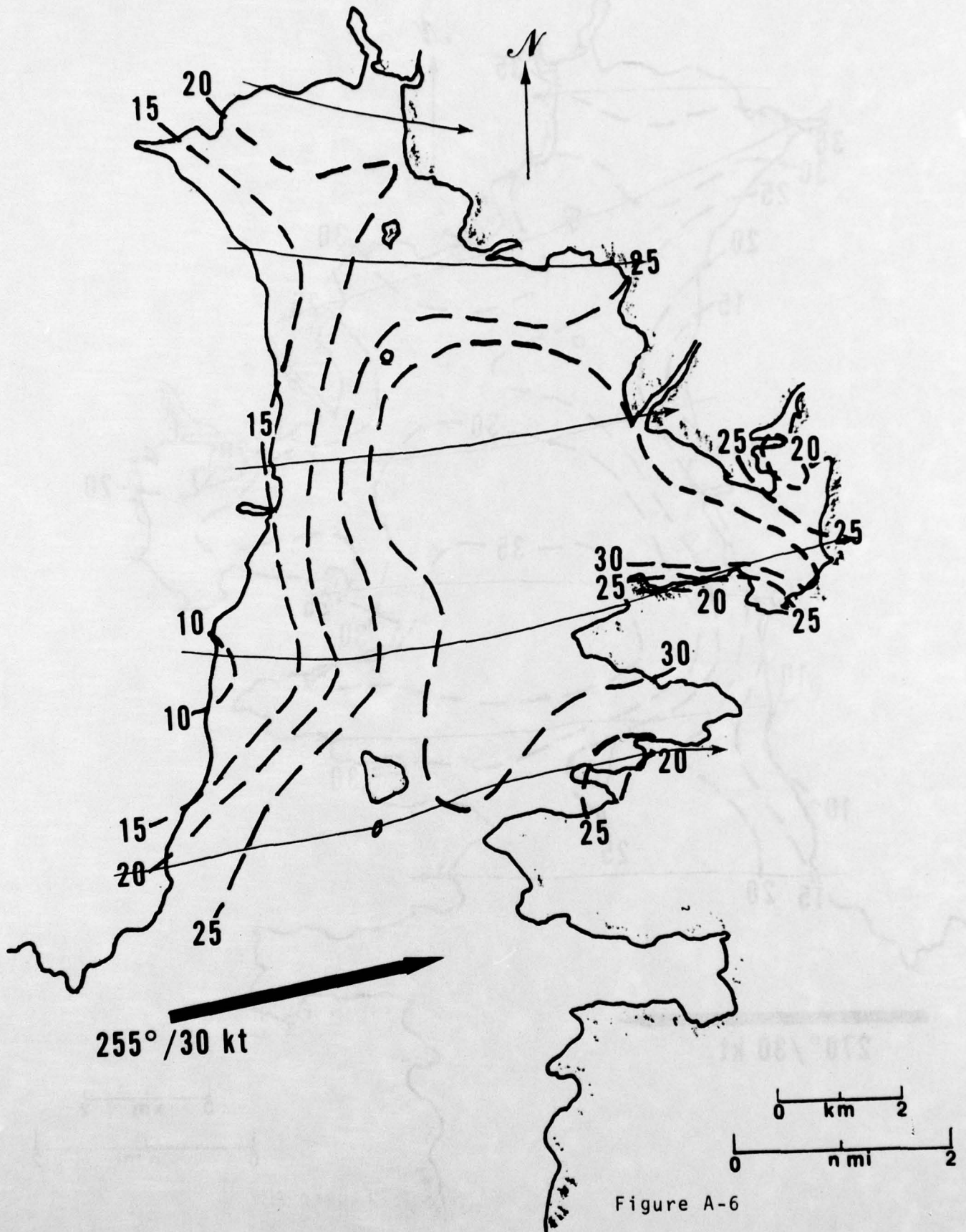


Figure A-6

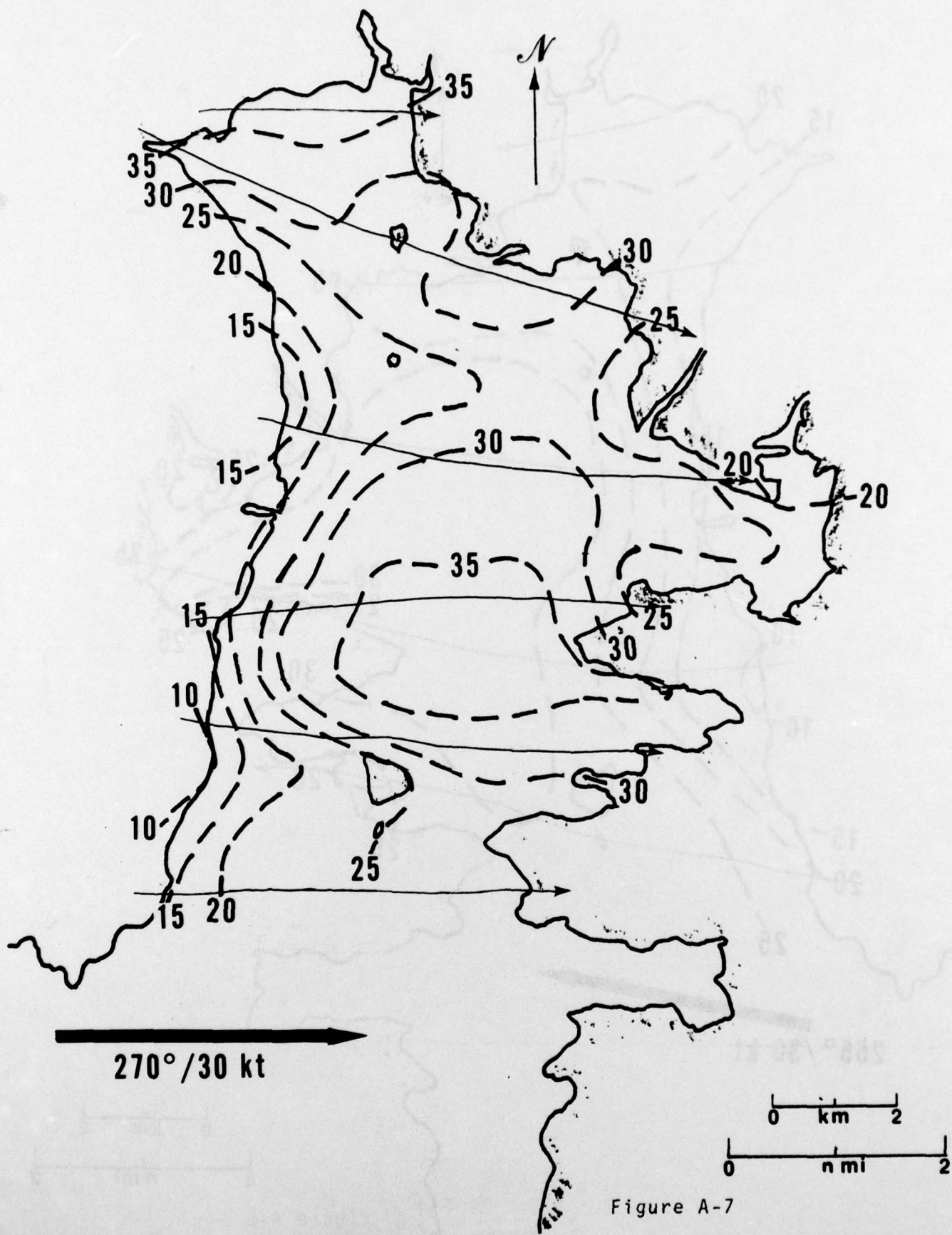


Figure A-7

APPENDIX B

STREAMLINE AND MAXIMUM GUST DISTRIBUTIONS

Streamline and maximum gust distributions (in kt) from the wind tunnel laboratory experiment as a function of varying wind direction are shown in Figures B-1 through B-7. Gust values are for a 70 ft elevation; incoming wind speed is 30 kt.

<u>Figure Number</u>	<u>Wind Direction From</u>
B-1	180°
B-2	195°
B-3	210°
B-4	225°
B-5	240°
B-6	255°
B-7	270°

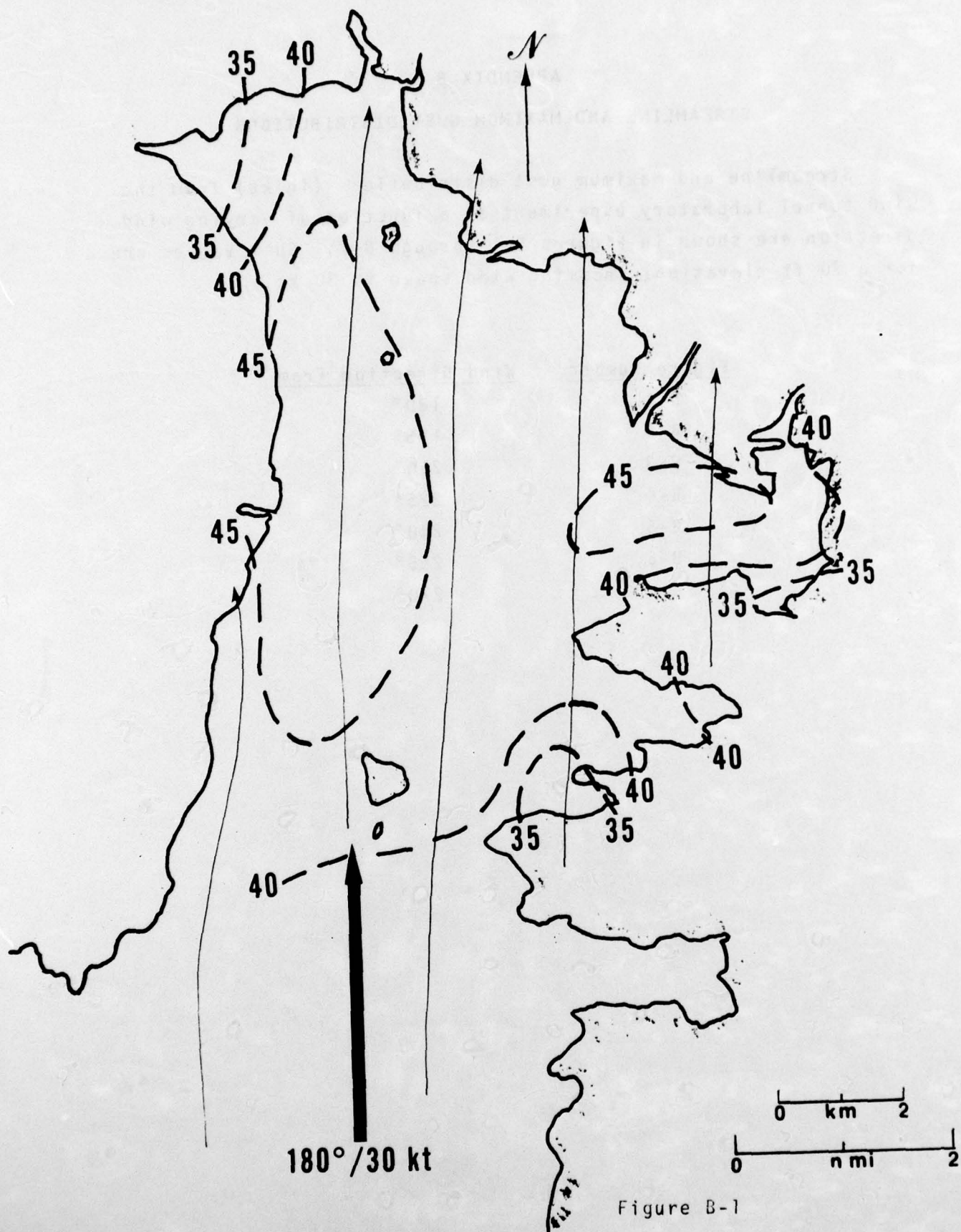


Figure B-1

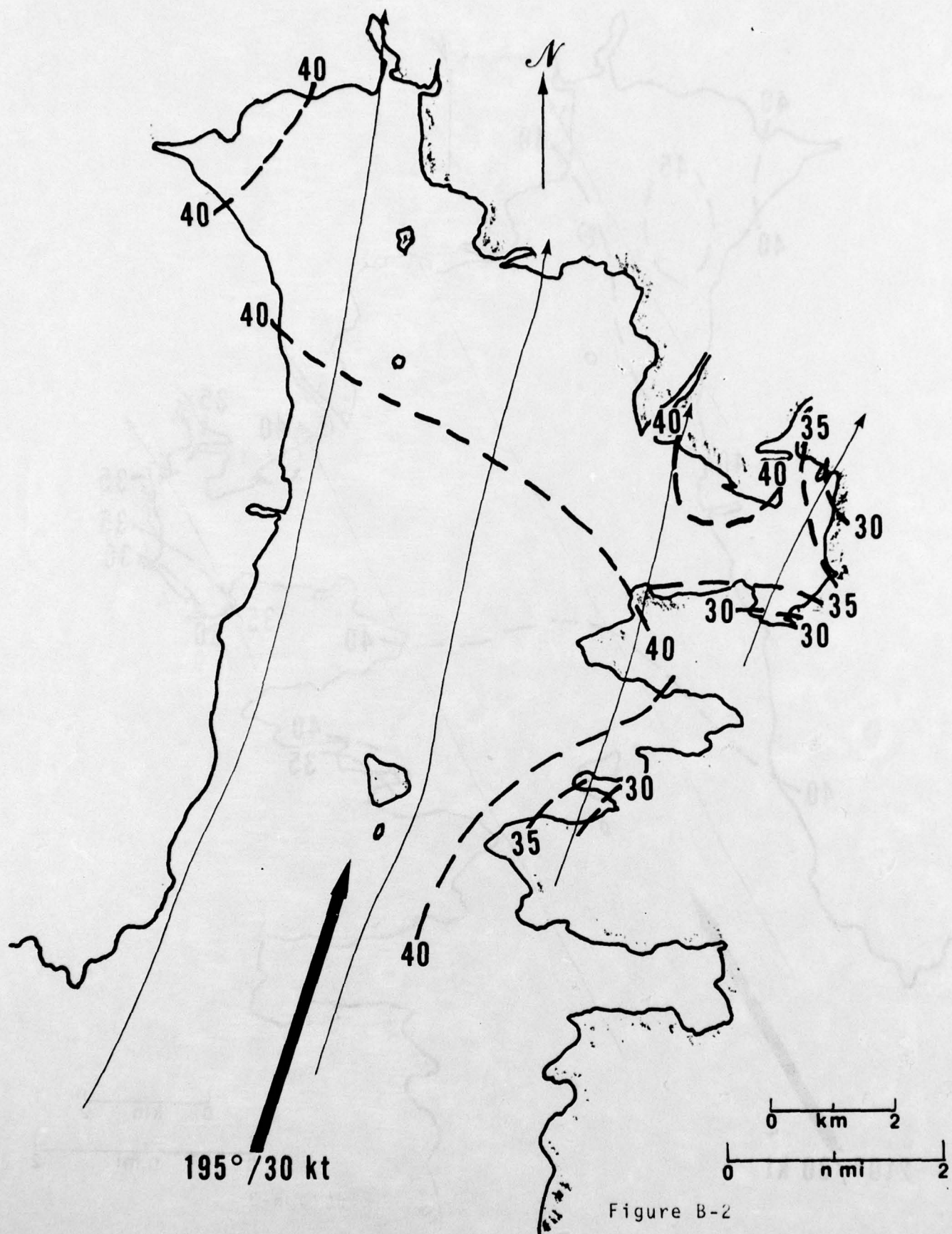
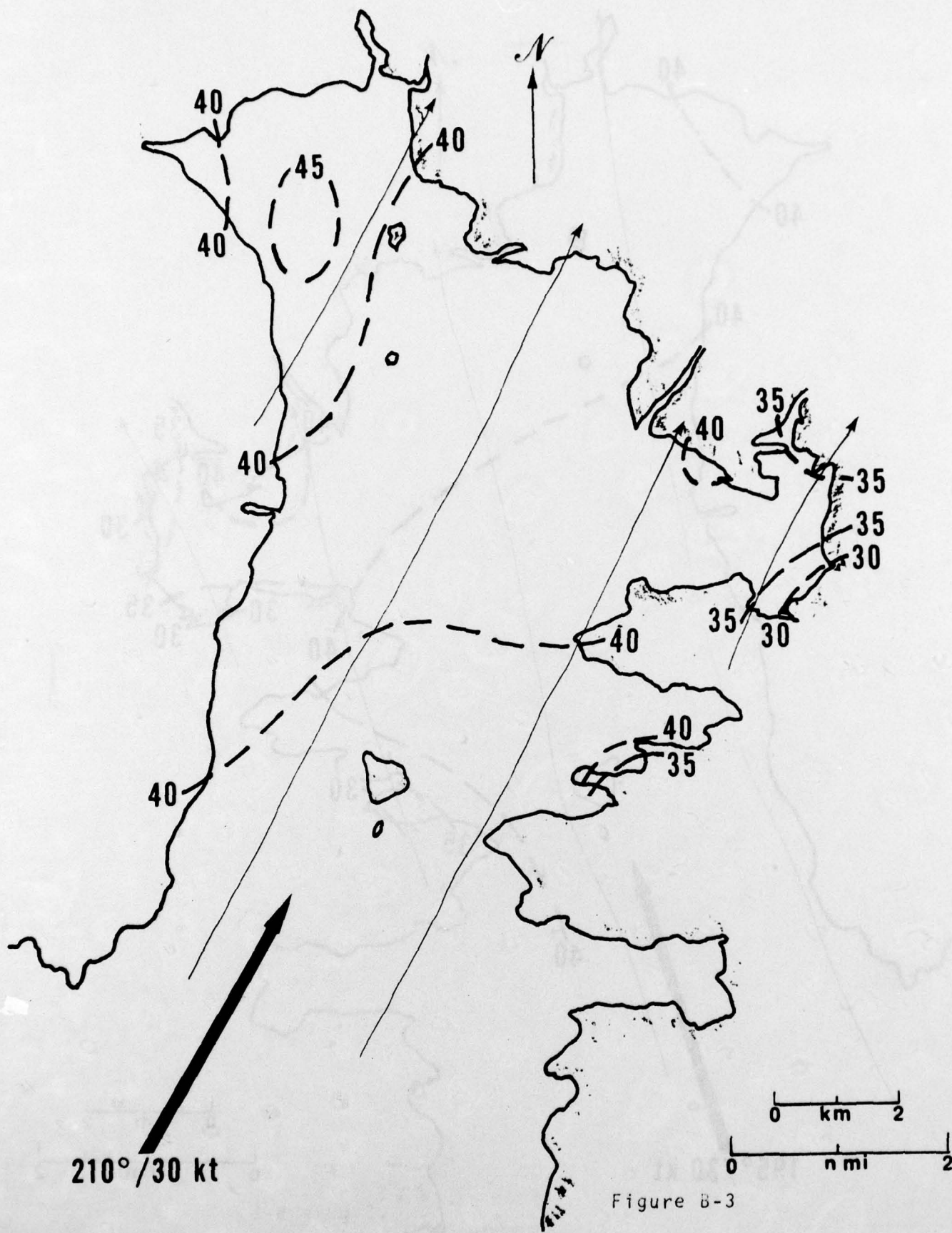
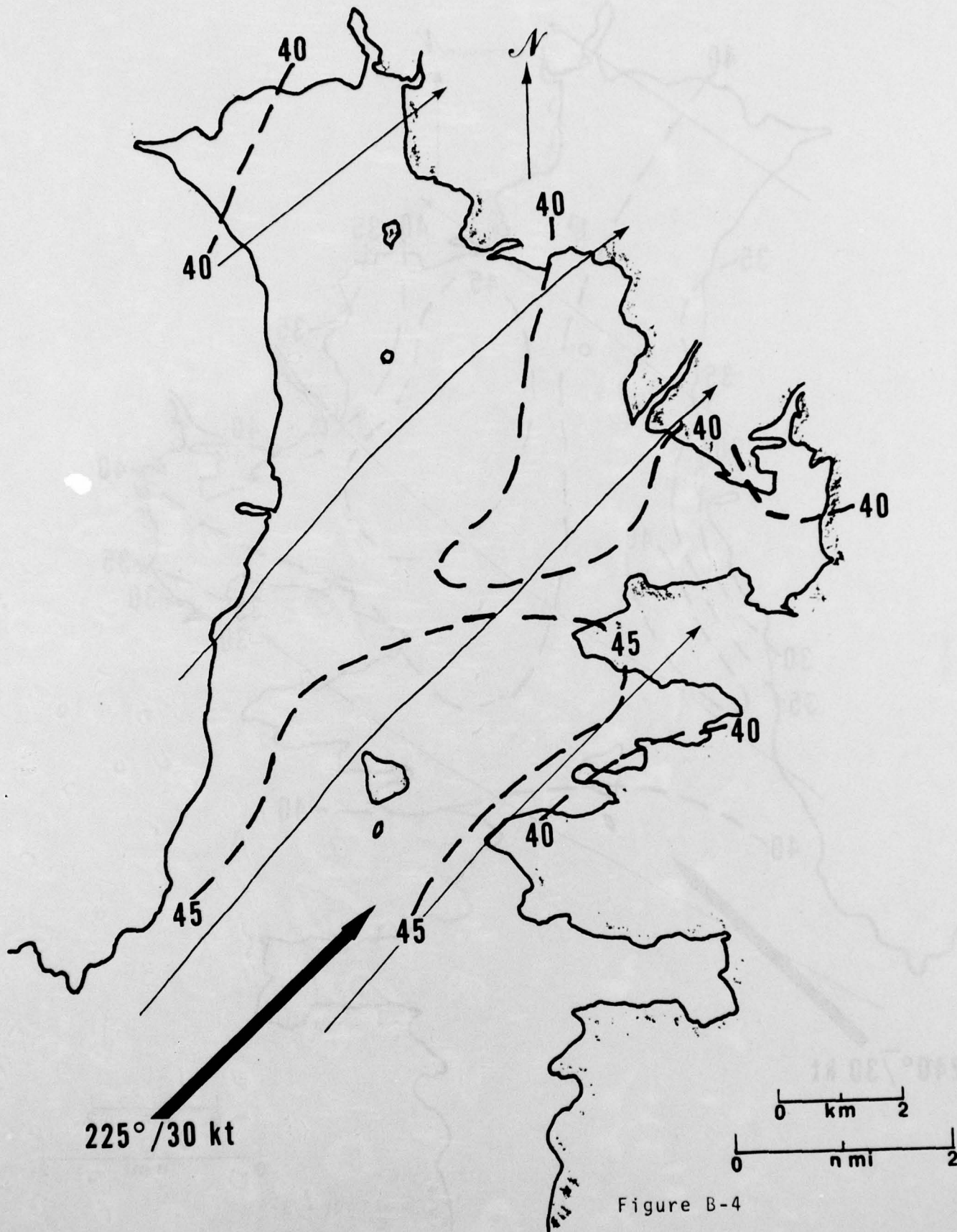


Figure B-2





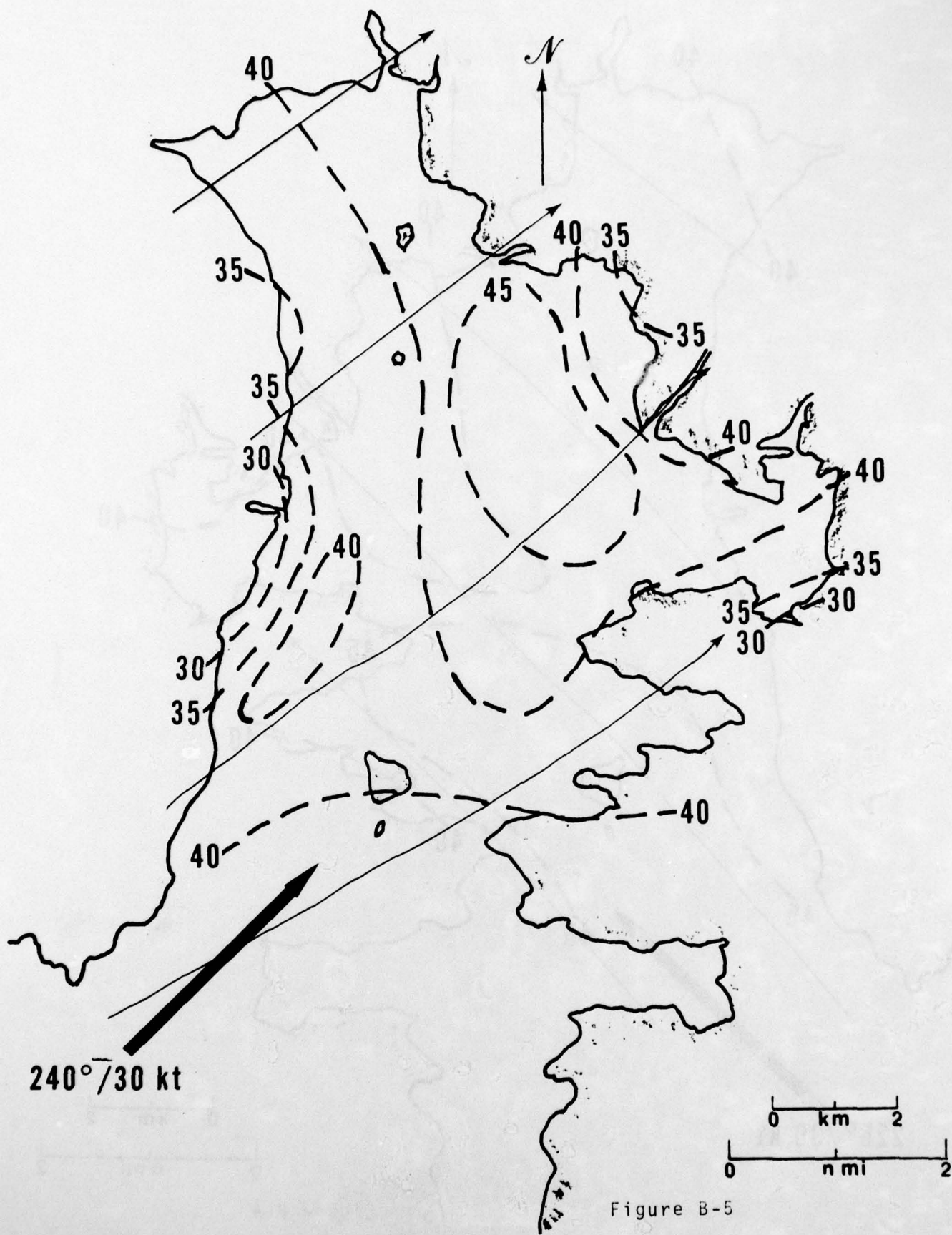


Figure B-5

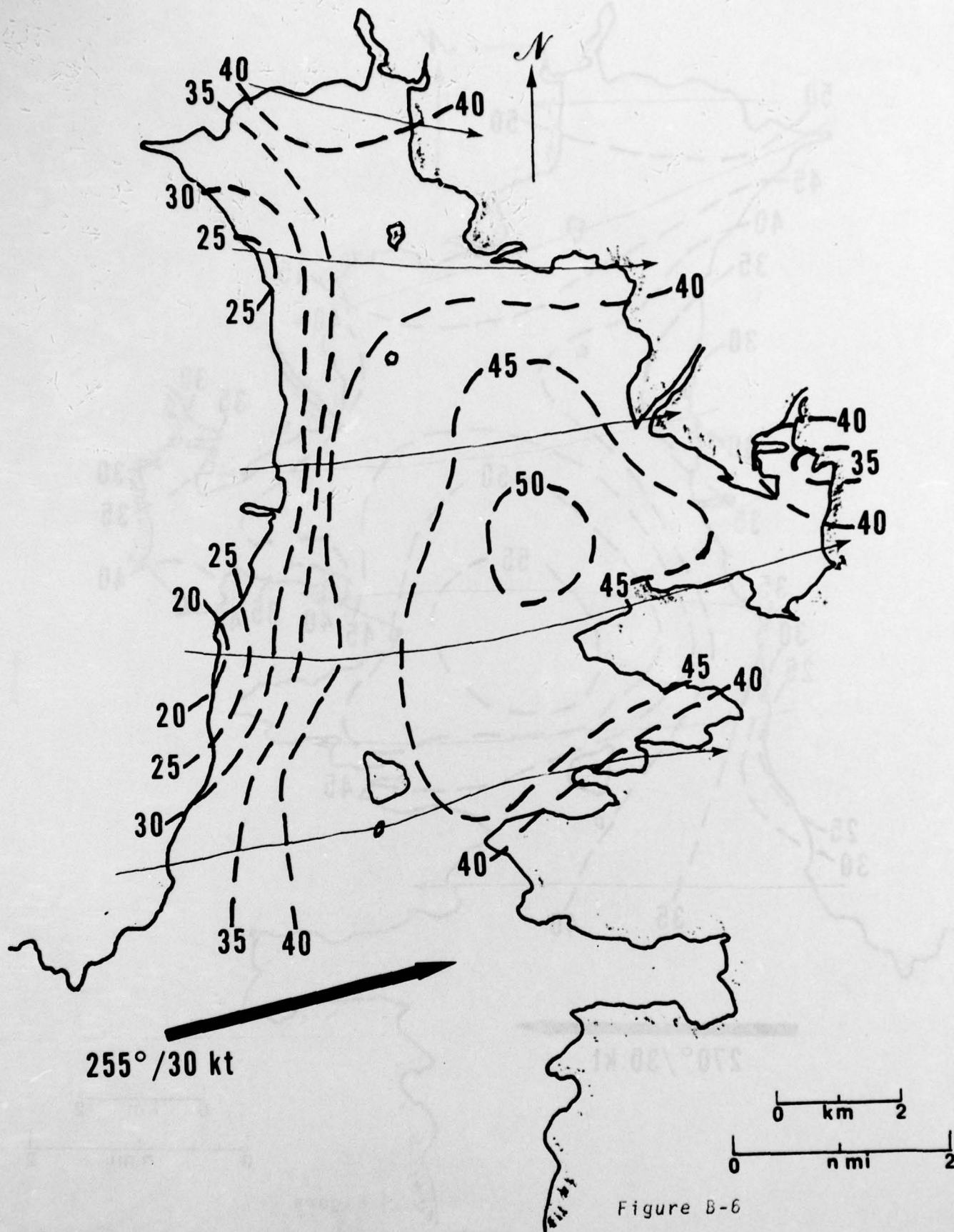


Figure B-6

